

# Output Embedding Centering for Stable LLM Pretraining

Felix Stollenwerk  
AI Sweden

Anna Lokrantz  
AI Sweden

Niclas Hertzberg  
AI Sweden

## Abstract

Pretraining of large language models is not only expensive but also prone to certain training instabilities. A specific instability that often occurs at the end of training is output logit divergence. The most widely used mitigation strategies, z-loss and logit soft-capping, merely address the symptoms rather than the underlying cause of the problem. In this paper, we analyze the instability from the perspective of the output embeddings' geometry and identify anisotropic embeddings as its source. Based on this, we propose *output embedding centering* (OEC) as a new mitigation strategy, and demonstrate that it suppresses output logit divergence. OEC can be implemented in two different ways: as a deterministic operation called  $\mu$ -centering, or a regularization method called  $\mu$ -loss. Our experiments show that both variants outperform z-loss in terms of training stability, while being on par with logit soft-capping. This holds true both in the presence and the absence of weight tying. As a secondary result, we find that  $\mu$ -loss is significantly less sensitive to regularization hyperparameter tuning than z-loss.

## 1 Introduction

Large language models (LLMs) have shown great promise for solving many different types of tasks. However, instability during the most computationally expensive phase of pretraining LLMs is a recurring issue (Chowdhery et al., 2022; Takase et al., 2025; Dehghani et al., 2023), often resulting in a significant amount of wasted compute. There are several types of training instabilities, e.g. extremely large attention logits (Dehghani et al., 2023) or divergence of the output logits in the language modeling head (Chowdhery et al., 2022). Wortsman et al. (2023) have shown that these training instabilities can be reproduced in a proxy setting of small-scale models in combination with high learning rates. This allows to study the effect of mitigation strategies in isolation<sup>1</sup> on a small scale, and draw conclusions for large-scale pretraining. In this work, we adopt their approach and specifically address the problem of output logit divergence.

**Language Modeling Head** We consider decoder-only Transformer models (Vaswani et al., 2017; Radford et al., 2018), in which the language modeling head is the final component responsible for mapping the final hidden state to a probability distribution over the tokens in the vocabulary. Following the notation of Stollenwerk & Stollenwerk (2025), the standard language modeling head is defined by the following equations:

$$\mathcal{L} = -\log(p_t) \tag{1}$$

$$p_t = \frac{\exp(l_t)}{\sum_{j=1}^V \exp(l_j)} \tag{2}$$

$$l_i = e_i \cdot h \tag{3}$$

$\mathcal{L} \in \mathbb{R}_{\geq 0}$  is the loss for next token prediction, while  $p_t \in [0, 1]$  represents the probability assigned to the true token  $t \in \mathcal{V}$ . Here,  $\mathcal{V} \equiv \{1, \dots, V\}$ , where  $V$  is the size of the vocabulary.

<sup>1</sup>In particular, weight decay, which also mitigates the issue to some extent (Wortsman et al., 2023), is not applied to avoid interference.

The logits and output embeddings for each token  $i \in \mathcal{V}$  are denoted by  $l_i \in \mathbb{R}$  and  $e_i \in \mathbb{R}^H$ , respectively, with  $H$  being the dimension of the model’s hidden space. The final hidden state is given by  $h \in \mathbb{R}^H$ . The output embeddings  $e_i$  can either be learned independently or tied to the input embeddings (Press & Wolf, 2017).

**Mitigation Strategies** The most widely adopted solution to the problem of divergent output logits is *z-loss*, introduced by Chowdhery et al. (2022). Denoting the denominator of Eq. (2) by

$$Z := \sum_{j=1}^V \exp(l_j) \quad (4)$$

*z-loss* adds a regularization term of the form

$$\mathcal{L}_z := 10^{-4} \cdot \log^2(Z) \quad (5)$$

It has proven an effective measure to prevent the logits from diverging and stabilize the training process, also in the proxy setting of Wortsman et al. (2023). Consequently, *z-loss* has been utilized in several recent models (Team OLMo et al., 2025; Chameleon Team, 2025; Wang et al., 2022; Team OLMo & Allen Institute for AI, 2025). Similarly, Baichuan 2 (Yang et al., 2025) introduced a variant of *z-loss*, *max-z loss*, that penalizes the square of the maximum logit value. In contrast to adding auxiliary losses, Gemma 2 (Gemma Team et al., 2024) enforces bounds via “logit soft-capping”

$$l_i \leftarrow c \cdot \tanh(l_i/c) \quad (6)$$

which is applied between Eq. (2) and Eq. (3). This model intervention confines the logits to a fixed numerical range determined by the hyperparameter  $c$  with default value  $c = 30$ . Another method, NormSoftMax (Jiang et al., 2023), proposes a dynamic temperature scaling in the softmax function based on the distribution of the logits. The above methods all have in common that they address the symptoms rather than the cause of output logit divergence. In order to identify the cause, we will examine the role of the output embeddings<sup>2</sup>, which affect the output logits via Eq. (3).

**Anisotropic Embeddings** A well-known phenomenon exhibited by the embeddings of Transformer models is that they typically do not distribute evenly across the different dimensions in hidden space. This problem of anisotropy was first described by Gao et al. (2019). At the time, the understanding was that the embeddings occupy a narrow cone in hidden space. Several regularization methods have been proposed to mitigate the problem, e.g. cosine regularization (Gao et al., 2019), Laplace regularization (Zhang et al., 2020) and spectrum control (Wang et al., 2020). Biś et al. (2021) showed that embeddings are actually near-isotropic around their center, and argued that the observed anisotropy is mainly due to a common shift of the embeddings away from the origin. Recently, Stollenwerk & Stollenwerk (2025) identified the root cause of this phenomenon; they showed that it is the second moment in Adam that causes the common shift of the embeddings and suggested Coupled Adam as an optimizer-based mitigation strategy. Furthermore, their analysis reveals that the phenomenon stems from the output embeddings rather than the input embeddings, in accordance with the observations reported in Machina & Mercer (2024).

**Our Contributions** This paper provides the following contributions.

- *Analysis:* We combine the above two lines of research and analyze the role of anisotropic embeddings in causing output logit divergence.
- *Methods:* We suggest output embedding centering (OEC), a theoretically founded mitigation strategy with two implementations,  $\mu$ -centering and  $\mu$ -loss, that both keep the output embeddings and logits centered around zero.

<sup>2</sup>The final hidden states are arguably less relevant in this context, as they are usually normalized.

- *Training Stability*: We show experimentally that our methods, compared to z-loss and logit soft-capping, lead to an equal or better learning rate sensitivity in the small-scale proxy setting of Wortsman et al. (2023). This feature is expected to transfer to (more) effective stabilization of large-scale LLM pretraining.
- *Hyperparameter Sensitivity*: Our regularization method  $\mu$ -loss is significantly less sensitive to the regularization hyperparameter, while z-loss requires careful hyperparameter tuning. Furthermore, our results indicate that the optimal hyperparameter for z-loss is larger than previously assumed.

## 2 Output Embedding Centering

In this section, we attempt to identify and address the root cause of output logit divergence. First, the impact of the output embeddings on the logits is studied. Based on our findings, we present two related methods that center the output embeddings to suppress logit divergence,  $\mu$ -centering and  $\mu$ -loss.

### 2.1 Output Embeddings and Logits

We examine the relationship between the output embeddings  $e_i$  and logits  $l_i$ . In particular, we consider their means and ranges. This will serve as a basis for the subsequent introduction of our output embedding centering methods. The connection between the mean word embedding

$$\mu = \frac{1}{V} \sum_{i=1}^V e_i \quad (7)$$

and the mean logit

$$\bar{l} = \frac{1}{V} \sum_{i=1}^V l_i \quad (8)$$

is expressed by the following lemma.

**Lemma 1.** *The mean logit is proportional to the mean embedding:*

$$\bar{l} = \mu \cdot h \quad (9)$$

*Proof.*

$$\bar{l} \stackrel{(3)}{=} \frac{1}{V} \sum_{i=1}^V (e_i \cdot h) = \left( \frac{1}{V} \sum_{i=1}^V e_i \right) \cdot h \stackrel{(7)}{=} \mu \cdot h$$

Note that in the second step, the linearity of the dot product was used.  $\square$

The impact of the word embeddings on the range of the logits is summarized by the following lemma.

**Lemma 2.** *The logits  $l_j$  are globally bounded by*

$$-\max_i \|e_i\| \cdot \|h\| \leq l_j \leq \max_i \|e_i\| \cdot \|h\| \quad (10)$$

*Proof.* A single logit is given by  $l_j \stackrel{(3)}{=} e_j \cdot h = \|e_j\| \|h\| \cos \alpha_j$ , where  $\alpha_j$  is the angle between  $e_j$  and  $h$ . Hence, it is individually bounded by  $-\|e_j\| \cdot \|h\| \leq l_j \leq \|e_j\| \cdot \|h\|$ . This leads to the global bounds in Eq. (10).  $\square$

In summary, the mean output embedding directly impacts the mean logit, and the norms of the output embeddings define the range of the logits. Hence, controlling the output

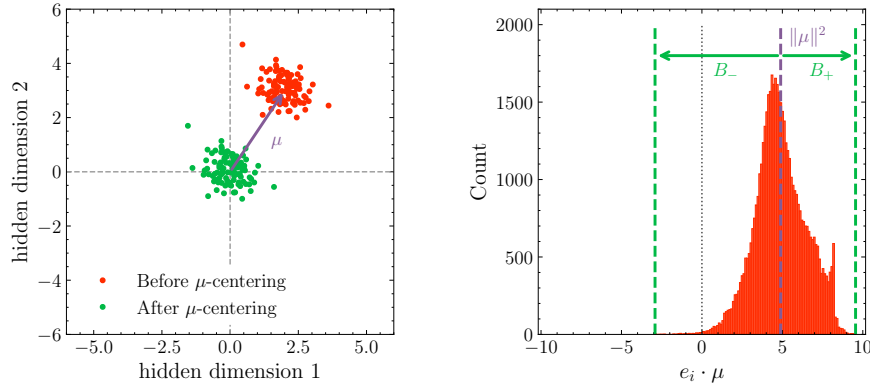


Figure 1: *Left*: Illustration of anisotropic embeddings and the effect of  $\mu$ -centering. The purple arrow represents the mean embedding  $\mu$ . *Right*: Histogram of dot products  $e_i \cdot \mu$  for a trained model with a standard language modeling head. The dotted, black line represents 0, while the purple and green dashed lines indicate  $\|\mu\|^2 = 4.9$  and the extrema of the dot product, respectively. In the example, we have  $B_- = 7.8$  and  $B_+ = 4.7$ , which means that the condition for reduced output logit bounds, Eq. (14), is fulfilled:  $B_{\text{ratio}} = 0.82 \leq 1$ .

embeddings provides a means to control the logits. This insight lays the foundation for *output embedding centering* (OEC). The idea behind OEC is to ensure that the mean output embedding  $\mu$  (cf. Eq. (7)) is bound to the origin, suppressing the common shift of the embeddings (cf. Sec. 1) and uncontrolled logit growth. OEC comes in two variants,  $\mu$ -centering and  $\mu$ -loss, which we will introduce next.

## 2.2 $\mu$ -centering

OEC can be implemented in a deterministic, hyperparameter-free manner by subtracting the mean output embedding  $\mu$  from each output embedding  $e_i$ , creating new output embeddings  $e_i^*$  after each optimization step:

$$e_i^* = e_i - \mu \quad (11)$$

This variant, called  $\mu$ -centering, is illustrated in the center panel of Fig. 1. It has some simple implications that can be summarized as follows:

**Proposition 3.** *Let  $l$  and  $\bar{l}^*$  denote the mean output logits before and after  $\mu$ -centering, respectively.*

- (i) *The mean output logit after  $\mu$ -centering is zero:  $\bar{l}^* = 0$*
- (ii) *The output logits standard deviation is not affected by  $\mu$ -centering:  $\sigma_{l^*} = \sigma_l$*
- (iii) *The output probabilities and the loss are not affected by  $\mu$ -centering.*

*Proof.* (i) Follows from Lemma 1 and Eq. (11). (ii) Follows from the shift-invariance of the standard deviation. (iii) Follows from the shift-invariance of the softmax in Eq. (2).  $\square$

However,  $\mu$ -centering also has a less obvious, yet considerably more important, effect: it reduces the global logits bound subject of Lemma 2, thereby suppressing the unlimited growth of  $|l_i|$  that can lead to divergences. Before we formalize this statement in Theorem 4, let us introduce some notation and build up an intuition for how this works in detail. We start by considering the dot products  $e_i \cdot \mu$  between each individual output embedding  $e_i$  and the mean output embedding  $\mu$ . A histogram of these dot products is shown on the right hand side of Fig. 1. As one can see, the typical distribution of the dot products approximates a skewed normal distribution centered around  $\|\mu\|^2$ . More importantly, it is bounded between  $\|\mu\|^2 - B_-$  and  $\|\mu\|^2 + B_+$  for some suitably chosen positive parameters  $B_-$  and  $B_+$ . Under certain conditions (to be specified below),  $\mu$ -centering reduces the bounds for

the dot products. This in turn leads to reduced bounds for the norm of the embeddings and the output logits. We will concretize and formalize this in the following theorem now.

**Theorem 4.** Let  $B_-, B_+ \in \mathbb{R}$  be bounds such that

$$\|\mu\|^2 - B_- \leq e_i \cdot \mu \leq \|\mu\|^2 + B_+ \quad (12)$$

where  $\mu$  represents the mean output embedding. Define the (non-negative) ratio

$$B_{\text{ratio}} = \frac{\max(B_-, B_+)}{\max(B_- - \|\mu\|^2, B_+ + \|\mu\|^2)} \quad (13)$$

and denote the output logits after  $\mu$ -centering by  $l_i^*$ . Then

$$B_{\text{ratio}} \leq 1 \iff \max |l_i^*| \leq \max |l_i| \quad (14)$$

The proof can be found in App. B. Importantly, the condition on  $B_{\text{ratio}}$  in Eq. (14) is empirically fulfilled for all our experiments with the standard language modeling head that are prone to output logit divergence, see App. C.

### 2.3 $\mu$ -loss

Instead of  $\mu$ -centering, we can also enforce OEC approximately by adding a regularization  $\mu$ -loss of the form

$$\mathcal{L}_\mu = \lambda \cdot \mu \cdot \mu \quad (15)$$

Here,  $\lambda \in \mathbb{R}^+$  is a hyperparameter that is set to

$$\lambda = 10^{-4} \quad (16)$$

by default, as in the case of z-loss (see Eq. (5)). While  $\mu$ -loss may offer more flexibility,  $\mu$ -centering has the advantage of being hyperparameter-free and deterministic.

### 2.4 Comparison to Existing Mitigation Strategies

We conclude this section by comparing the presented OEC methods,  $\mu$ -centering and  $\mu$ -loss, with the most widely used existing mitigation strategies, logit soft-capping and z-loss (Sec. 1). Logit soft-capping stands out as the only method that represents a model intervention, i.e. an adjustment of the model architecture. The other methods, in contrast, leave the model architecture unchanged and intervene in the training process instead. z-loss, on the other hand, is exceptional in the sense that it does not suppress positive and negative output logit divergences equally. This can easily be seen by considering  $\mathcal{L}_z$  as a function of a single logit  $l_i$ , with all other logits fixed:

$$\mathcal{L}_z(l_i) \stackrel{(4,5)}{\propto} \log^2 \left( \exp(l_i) + \sum_{j \neq i} \exp(l_j) \right) \quad (17)$$

Given that the sum over  $j \neq i$  is positive, this function is clearly non-symmetric:

$$\mathcal{L}_z(l_i) \neq \mathcal{L}_z(-l_i) \quad (18)$$

We refer the reader to App. D for illustrations. The other methods, however, treat positive and negative divergences similarly. Logit soft-capping, for instance, uses an odd function (see Eq. 6), while  $\mu$ -loss is quadratic in  $\mu$  (see Eq. 15) and thus invariant under  $\mu \rightarrow -\mu$  and  $\bar{l} \rightarrow -\bar{l}$ . Tab. 1 summarizes the means by which the discussed mitigation strategies prevent logit divergence. The general theoretical advantages of  $\mu$ -loss and  $\mu$ -centering are their simplicity and the fact that they have a theoretical foundation that addresses the root cause of the problem. In addition, they suppress positive and negative divergences equally (unlike z-loss), and pose a minimal interference only at training time, without changing the model itself (unlike logit soft-capping).

| name               | intervention | means                       | symmetry |
|--------------------|--------------|-----------------------------|----------|
| logit soft-capping | model        | element-wise transformation | yes      |
| z-loss             | training     | loss regularization         | no       |
| $\mu$ -loss        | training     | loss regularization         | yes      |
| $\mu$ -centering   | training     | parameter shift             | yes      |

Table 1: Overview of methods and means by which logit divergences are suppressed. Symmetry refers to whether positive and negative output logit divergences are treated equally.

### 3 Experiments

Our approach to studying training stability with regard to output logit divergence primarily follows the small-scale proxy setup from [Wortsman et al. \(2023\)](#). In particular, we train dense decoder models with a modern Transformer architecture ([Vaswani et al., 2017](#)) on 13.1 billion tokens for 100000 steps, using 7 different learning rates:

$$\eta \in \{3e-4, 1e-3, 3e-3, 1e-2, 3e-2, 1e-1, 3e-1\} \quad (19)$$

However, there are also a number of differences. We use FineWeb ([Penedo et al., 2024](#)) and the GPT-2 tokenizer ([Radford et al., 2019](#)) with a vocabulary size of  $V = 50304$ . Our 5 model sizes,

$$N \in \{16M, 29M, 57M, 109M, 221M\} \quad (20)$$

and the corresponding specifications (e.g. widths, number of layers and attention heads) are taken from [Porian et al. \(2024\)](#). The experiments are conducted with and without weight tying:

$$\text{weight tying} \in \{\text{false}, \text{true}\} \quad (21)$$

In addition, we use SwiGLU hidden activations ([Shazeer, 2020](#)) and a non-truncated Xavier weight initialization ([Glorot & Bengio, 2010](#)). Further details on model architecture and hyperparameters are provided in App. A. For each of the  $7 \times 5 \times 2 = 70$  combinations of learning rate, model size and weight tying defined by Eq. (19)-(21), we train five different models: A baseline model with the standard language modeling head, and models using soft-capping, z-loss,  $\mu$ -loss as well as  $\mu$ -centering. In order to compare the variants, we consider the dependency of the test loss on the learning rate, and evaluate the learning rate sensitivity as defined in [Wortsman et al. \(2023\)](#):

$$\text{LRS} = \mathbb{E}_\eta \left[ \min(\mathcal{L}(\eta), \mathcal{L}_0) - \min_\eta \mathcal{L} \right] \quad (22)$$

Here,  $\eta$  are the learning rates from Eq. (19) and  $\mathcal{L}_0$  denotes the loss at initialization time. This is done independently for each combination of model size and weight tying, Eq. (20) and (21). The learning rate sensitivity in this small-scale setting has been shown to be a valuable proxy for training stability in the large-scale setting ([Wortsman et al., 2023](#)). Additionally, we investigate the dependency of a few other metrics on the learning rate for the purpose of analyzing the functionality of the different methods. Firstly, we consider the norm  $\|\mu\|$  of the mean embedding (see Eq. (7)). Secondly, we compute sample estimates for the mean logit  $\bar{l}$  (see Eq. (8)), the logits standard deviation  $\sigma_l$  as well as the maximum absolute logit  $\max_j |l_j|$ , using  $5 \cdot 10^5$  logit vectors created from the test data. Finally, the time  $t$  to train a model on 4 A100 GPUs using data parallelism is compared.

### 4 Results

**Training Stability** The main results of our experiments without weight tying are shown in Tab. 2 and Fig. 2. The top table (i) demonstrates that the optimal loss  $\min_\eta \mathcal{L}$  for each model size is virtually the same for all methods. As expected, the top figure shows that the non-regularized baseline is the first to diverge with larger learning rates. Interestingly, z-loss leads to occasional divergences as well, given a large enough learning rate<sup>3</sup>. Meanwhile,

<sup>3</sup>At first glance, this might seem to contradict the results from [Wortsman et al. \(2023\)](#). However, a thorough look at their Fig. 3 reveals a similar behavior for z-loss.

| (i) Optimal Loss ( $\downarrow$ ) |             |             |             |             |              |
|-----------------------------------|-------------|-------------|-------------|-------------|--------------|
| $N$                               | baseline    | soft-c.     | z-loss      | $\mu$ -loss | $\mu$ -cent. |
| 16M                               | <b>3.84</b> | <b>3.84</b> | <b>3.84</b> | <b>3.84</b> | <b>3.84</b>  |
| 29M                               | 3.59        | <b>3.58</b> | <b>3.58</b> | 3.59        | <b>3.58</b>  |
| 57M                               | 3.37        | <b>3.36</b> | 3.37        | 3.37        | 3.37         |
| 109M                              | 3.20        | <b>3.19</b> | 3.20        | 3.20        | 3.20         |
| 221M                              | 3.05        | <b>3.04</b> | 3.05        | 3.05        | 3.05         |

| (ii) Learning Rate Sensitivity ( $\downarrow$ ) |          |              |        |              |              |
|---|----------|--------------|--------|--------------|--------------|
| $N$   | baseline | soft-c.      | z-loss | $\mu$ -loss  | $\mu$ -cent. |
| 16M   | 0.306    | 0.032        | 0.054  | 0.031        | <b>0.028</b> |
| 29M   | 0.391    | <b>0.024</b> | 0.033  | 0.027        | 0.029        |
| 57M   | 0.508    | 0.035        | 0.235  | <b>0.031</b> | 0.041        |
| 109M  | 0.344    | 0.050        | 0.118  | <b>0.046</b> | 0.051        |
| 221M  | 0.412    | 0.073        | 0.109  | <b>0.056</b> | 0.061        |

| (iii) Additional Training Time ( $\downarrow$ ) |          |         |        |             |              |
|---|----------|---------|--------|-------------|--------------|
| $N$   | baseline | soft-c. | z-loss | $\mu$ -loss | $\mu$ -cent. |
| 16M   | 0.0%     | 10.0%   | 6.4%   | <b>0.4%</b> | 0.6%         |
| 29M   | 0.0%     | 6.4%    | 4.3%   | 0.7%        | <b>0.5%</b>  |
| 57M   | 0.0%     | 3.9%    | 2.5%   | 0.6%        | <b>0.4%</b>  |
| 109M  | 0.0%     | 2.0%    | 1.5%   | <b>0.4%</b> | <b>0.4%</b>  |
| 221M  | 0.0%     | 0.7%    | 0.8%   | <b>0.2%</b> | 0.3%         |

Table 2: Main results for all model sizes and variants without weight tying. *From top to bottom:* (i) Optimal loss,  $\min_{\eta} \mathcal{L}$ . (ii) Learning rate sensitivity, LRS. (iii) Additional training time relative to baseline. In (i) and (ii), the best result for each model size is highlighted in bold. The same is true for (iii), where the baseline is excluded from the comparison though.

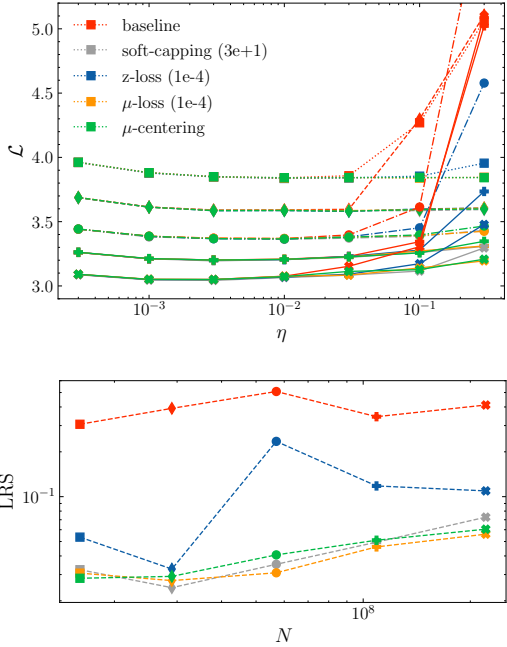


Figure 2: Main results for all model sizes and variants without weight tying. *Top:* Dependency of the loss  $\mathcal{L}$  on the learning rate  $\eta$ . *Bottom:* Dependency of the learning rate sensitivity LRS on the model size  $N$ .

none of the models using OEC or logit soft-capping diverge. This is also reflected in subtable (ii) of Tab. 2, which shows that these methods exhibit a lower learning rate sensitivity than z-loss, for all models sizes. In addition, subtable (iii) reveals that  $\mu$ -loss and  $\mu$ -centering are computationally cheap, such that the training time is minimally affected. The results for models using weight tying are very similar and shown in App. E.

**Analysis** The additional metrics mentioned at the end of Sec. 3 are visualized in Fig. 3. Firstly, regarding the logits mean (top left), we find that  $\mu$ -centering and  $\mu$ -loss center the logits at and around 0, respectively. Similarly, z-loss and logit soft-capping indirectly control the logits mean, although at negative values. In contrast, the logits mean diverges at higher learning rates for the baseline, in accordance with the loss divergence observed in Fig. 2. Secondly, the standard deviation (top right) is the same for  $\mu$ -centering and the baseline barring slight statistical differences, at least for lower learning rates for which the baseline training converges. This is consistent with the theoretical prediction, see Proposition 3. In contrast, z-loss and  $\mu$ -loss—since they are regularization methods—change the logit standard deviation slightly. The same holds for logit soft-capping, as it involves a non-linear transformation. Thirdly, the mean embedding norm is shown on the bottom left. As expected,  $\mu$ -centering maintains a norm of zero while both baseline and z-loss grow at higher learning rates, indicating that both z-loss and logit soft-capping fail to prevent anisotropic embeddings. Meanwhile,  $\mu$ -loss constrains the mean embedding norm to relatively small values. Finally, as predicted by Theorem 4, both  $\mu$ -centering and  $\mu$ -loss restrict the logit bound such that the maximum logit remains stable. Logit soft-capping achieves the same by design. z-loss also implicitly restricts the maximum logit, albeit to a lesser degree than our methods, which explains the divergence observed for training using z-loss. In contrast, the maximum logit grows extremely large for the baseline models. In summary, the results are in accordance with the theoretical predictions from Sec. 2.

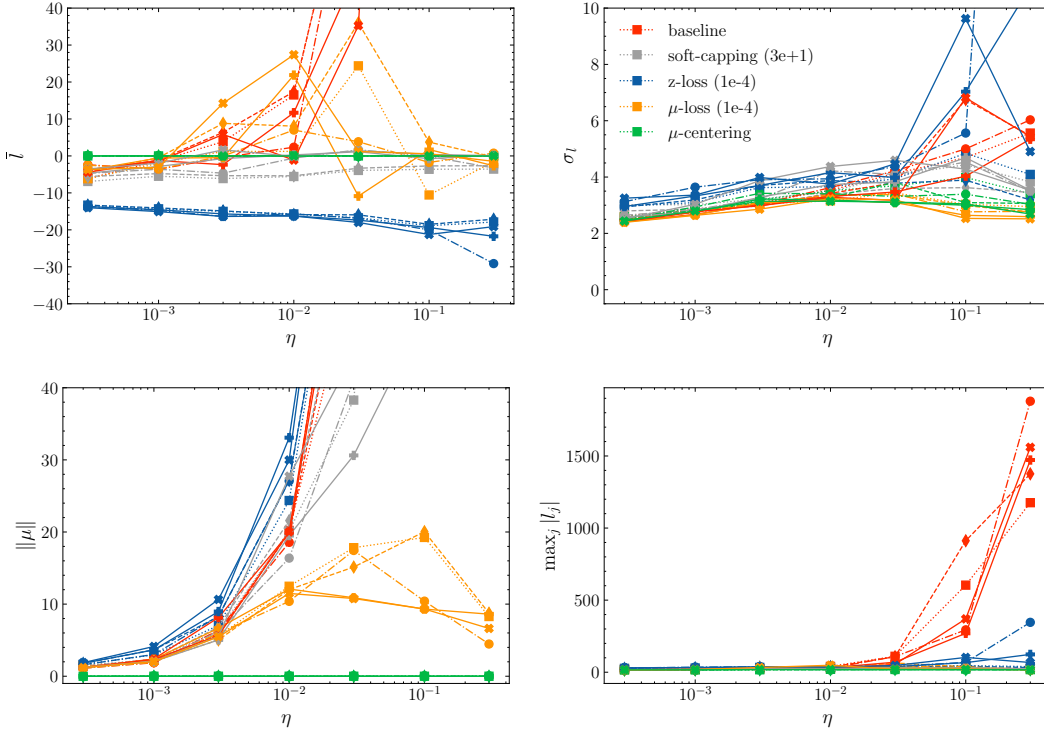


Figure 3: Additional results from the experiments without weight tying. The plots show the dependency of the logits mean (top left), logits standard deviation (top right), mean embedding norm (bottom left) and maximum absolute logit (bottom right) on the learning rate.

## 5 Hyperparameter Sensitivity

So far, the regularization hyperparameters have been set to their default value  $\lambda = 10^{-4}$  for both regularization methods, z-loss (cf. Eq. (5)) and  $\mu$ -loss (cf. Eq. (16)). We now vary the regularization hyperparameter

$$\lambda \in \{10^{-7}, 10^{-4}, 10^{-1}, 10^2\} \quad (23)$$

for those methods, and determine the optimal loss and learning rate sensitivity as in Sec. 4 for each choice of  $\lambda$ . The results are presented in Tab. 3 and Fig. 4. For  $\mu$ -loss, hyperparameter tuning is notably straightforward: the regularization coefficient only needs to be sufficiently large to enforce the centering effect. In fact, for larger values ( $\lambda \geq 10^{-4}$ ), the training is stable and does not exhibit a strong dependency on the exact value of  $\lambda$ . Only when  $\lambda$  is too small ( $\lambda = 10^{-7}$ ), we observe that the loss diverges for large learning rates across all model sizes. This behavior stands in contrast to z-loss, which requires more careful tuning. Severe divergences appear for  $\lambda = 10^2$ , but also for lower values of  $\lambda$  in conjunction with large learning rates. Our results indicate that the optimal value for z-loss is  $\lambda = 10^{-1}$ , which is significantly larger than the previously assumed optimal value of  $10^{-4}$ . Importantly, however, even for the optimal  $\lambda$ , z-loss is outperformed by both  $\mu$ -loss and  $\mu$ -centering. This performance gap is evident in the learning rate sensitivity values for the largest model size  $N = 221$  in Tab. 3, as well as in the comparison of the rightmost points—corresponding to the largest model size—across the learning rate sensitivity plots in Fig. 4.

## 6 Conclusions

This paper establishes a link between the problems of anisotropic embeddings and output logit divergence. We have identified the former as the cause of the latter, and introduced

| $\mu$ -loss                       |             |             |             |             | $z$ -loss                         |           |           |             |        |
|-----------------------------------|-------------|-------------|-------------|-------------|-----------------------------------|-----------|-----------|-------------|--------|
| (i) Optimal Loss ( $\downarrow$ ) |             |             |             |             | (i) Optimal Loss ( $\downarrow$ ) |           |           |             |        |
| $N$                               | $10^{-7}$   | $10^{-4}$   | $10^{-1}$   | $10^2$      | $N$                               | $10^{-7}$ | $10^{-4}$ | $10^{-1}$   | $10^2$ |
| 16M                               | 3.84        | 3.84        | 3.84        | <b>3.81</b> | 16M                               | 3.84      | 3.84      | <b>3.83</b> | 4.19   |
| 29M                               | 3.59        | 3.59        | 3.58        | <b>3.56</b> | 29M                               | 3.59      | 3.58      | <b>3.57</b> | 3.94   |
| 57M                               | 3.37        | 3.37        | 3.37        | <b>3.36</b> | 57M                               | 3.37      | 3.37      | <b>3.35</b> | 3.79   |
| 109M                              | <b>3.20</b> | <b>3.20</b> | <b>3.20</b> | <b>3.20</b> | 109M                              | 3.20      | 3.20      | <b>3.18</b> | 3.64   |
| 221M                              | <b>3.05</b> | <b>3.05</b> | <b>3.05</b> | <b>3.05</b> | 221M                              | 3.05      | 3.05      | <b>3.03</b> | 3.49   |

| (ii) Learning Rate Sensitivity ( $\downarrow$ ) |           |              |              |              | (ii) Learning Rate Sensitivity ( $\downarrow$ ) |           |              |              |        |
|---|-----------|--------------|--------------|--------------|---|-----------|--------------|--------------|--------|
| $N$   | $10^{-7}$ | $10^{-4}$    | $10^{-1}$    | $10^2$       | $N$   | $10^{-7}$ | $10^{-4}$    | $10^{-1}$    | $10^2$ |
| 16M   | 0.182     | <b>0.031</b> | <b>0.031</b> | 0.054        | 16M   | 0.037     | 0.054        | <b>0.032</b> | 1.156  |
| 29M   | 0.052     | <b>0.027</b> | 0.034        | 0.040        | 29M   | 0.044     | <b>0.033</b> | 0.043        | 1.780  |
| 57M   | 0.110     | <b>0.031</b> | 0.038        | 0.033        | 57M   | 0.107     | 0.235        | <b>0.047</b> | 1.392  |
| 109M  | 0.125     | 0.046        | 0.048        | <b>0.034</b> | 109M  | 0.076     | 0.118        | <b>0.059</b> | 2.150  |
| 221M  | 0.129     | 0.056        | 0.056        | <b>0.055</b> | 221M  | 0.131     | 0.109        | <b>0.101</b> | 2.166  |

Table 3: Optimal Loss (top) and Learning Rate Sensitivity (bottom) for  $\mu$ -loss (left) and  $z$ -loss (right) with different regularization hyperparameters  $\lambda$  (specified in the column headers).

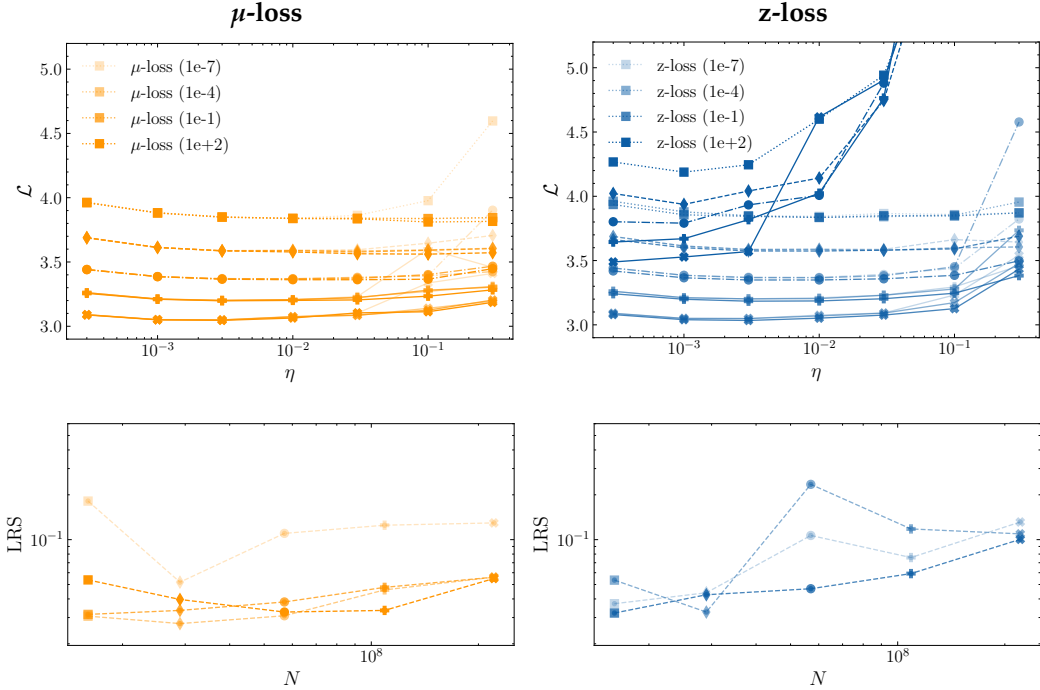


Figure 4: Hyperparameter dependency of  $\mu$ -loss (left) and  $z$ -loss (right). The top plots show loss  $\mathcal{L}$  vs. learning rate  $\eta$ , while the bottom plots show learning rate sensitivity vs. model size  $N$ . The results correspond to (i) and (ii) in Tab. 3, respectively.

output embedding centering (OEC) as a theoretically well-founded mitigation strategy. It can be implemented either in terms of the deterministic, hyperparameter-free method ( $\mu$ -centering), or a regularization method ( $\mu$ -loss). We have conducted systematic experiments comparing these methods to the two most widely used existing mitigation strategies,  $z$ -loss and logit soft-capping, in a small-scale setting that serves as a proxy for training stability at large. The results show that our methods outperform  $z$ -loss, while being on par with logit soft-capping. However, in contrast to the latter, our OEC methods avoid model intervention and are computationally cheaper. The code to reproduce our results is available at [github.com/flxst/output-embedding-centering](https://github.com/flxst/output-embedding-centering).

## References

- Daniel Biś, Maksim Podkorytov, and Xiuwen Liu. Too much in common: Shifting of embeddings in transformer language models and its implications. In *North American Chapter of the Association for Computational Linguistics (NAACL)*, 2021.
- Chameleon Team. Chameleon: Mixed-modal early-fusion foundation models, 2025. URL <https://arxiv.org/abs/2405.09818>.
- Aakanksha Chowdhery, Sharan Narang, Jacob Devlin, Maarten Bosma, Gaurav Mishra, Adam Roberts, Paul Barham, Hyung Won Chung, Charles Sutton, Sebastian Gehrmann, Parker Schuh, Kensen Shi, Sasha Tsvyashchenko, Joshua Maynez, Abhishek Rao, Parker Barnes, Yi Tay, Noam Shazeer, Vinodkumar Prabhakaran, Emily Reif, Nan Du, Ben Hutchinson, Reiner Pope, James Bradbury, Jacob Austin, Michael Isard, Guy Gur-Ari, Pengcheng Yin, Toju Duke, Anselm Levskaya, Sanjay Ghemawat, Sunipa Dev, Henryk Michalewski, Xavier Garcia, Vedant Misra, Kevin Robinson, Liam Fedus, Denny Zhou, Daphne Ippolito, David Luan, Hyeontaek Lim, Barret Zoph, Alexander Spiridonov, Ryan Sepassi, David Dohan, Shivani Agrawal, Mark Omernick, Andrew M. Dai, Thanumalayan Sankaranarayanan Pillai, Marie Pellat, Aitor Lewkowycz, Erica Moreira, Rewon Child, Oleksandr Polozov, Katherine Lee, Zongwei Zhou, Xuezhi Wang, Brennan Saeta, Mark Diaz, Orhan Firat, Michele Catasta, Jason Wei, Kathy Meier-Hellstern, Douglas Eck, Jeff Dean, Slav Petrov, and Noah Fiedel. Palm: Scaling language modeling with pathways, 2022. URL <https://arxiv.org/abs/2204.02311>.
- Mostafa Dehghani, Josip Djolonga, Basil Mustafa, Piotr Padlewski, Jonathan Heek, Justin Gilmer, Andreas Peter Steiner, Mathilde Caron, Robert Geirhos, Ibrahim Alabdulmohsin, Rodolphe Jenatton, Lucas Beyer, Michael Tschannen, Anurag Arnab, Xiao Wang, Carlos Riquelme Ruiz, Matthias Minderer, Joan Puigcerver, Utku Evci, Manoj Kumar, Sjoerd Van Steenkiste, Gamaleldin Fathy Elsayed, Aravindh Mahendran, Fisher Yu, Avital Oliver, Fantine Huot, Jasmijn Bastings, Mark Collier, Alexey A. Gritsenko, Vighnesh Birodkar, Cristina Nader Vasconcelos, Yi Tay, Thomas Mensink, Alexander Kolesnikov, Filip Pavetic, Dustin Tran, Thomas Kipf, Mario Lucic, Xiaohua Zhai, Daniel Keysers, Jeremiah J. Harmsen, and Neil Houlsby. Scaling vision transformers to 22 billion parameters. In Andreas Krause, Emma Brunskill, Kyunghyun Cho, Barbara Engelhardt, Sivan Sabato, and Jonathan Scarlett (eds.), *Proceedings of the 40th International Conference on Machine Learning*, volume 202 of *Proceedings of Machine Learning Research*, pp. 7480–7512. PMLR, 23–29 Jul 2023. URL <https://proceedings.mlr.press/v202/dehghani23a.html>.
- Jun Gao, Di He, Xu Tan, Tao Qin, Liwei Wang, and Tie-Yan Liu. Representation degeneration problem in training natural language generation models, 2019. URL <https://arxiv.org/abs/1907.12009>.
- Gemma Team, Morgane Riviere, Shreya Pathak, Pier Giuseppe Sessa, Cassidy Hardin, Surya Bhupatiraju, Léonard Hussenot, Thomas Mesnard, Bobak Shahriari, Alexandre Ramé, Johan Ferret, Peter Liu, Pouya Tafti, Abe Friesen, Michelle Casbon, Sabela Ramos, Ravin Kumar, Charline Le Lan, Sammy Jerome, Anton Tsitsulin, Nino Vieillard, Piotr Stanczyk, Sertan Girgin, Nikola Momchev, Matt Hoffman, Shantanu Thakoor, Jean-Bastien Grill, Behnam Neyshabur, Olivier Bachem, Alanna Walton, Aliaksei Severyn, Alicia Parrish, Aliya Ahmad, Allen Hutchison, Alvin Abdagic, Amanda Carl, Amy Shen, Andy Brock, Andy Coenen, Anthony Laforge, Antonia Paterson, Ben Bastian, Bilal Piot, Bo Wu, Brandon Royal, Charlie Chen, Chintu Kumar, Chris Perry, Chris Welty, Christopher A. Choquette-Choo, Danila Sinopalnikov, David Weinberger, Dimple Vijaykumar, Dominika Rogozińska, Dustin Herbison, Elisa Bandy, Emma Wang, Eric Noland, Erica Moreira, Evan Senter, Evgenii Eltyshev, Francesco Visin, Gabriel Rasskin, Gary Wei, Glenn Cameron, Gus Martins, Hadi Hashemi, Hanna Klimczak-Plucińska, Harleen Batra, Harsh Dhand, Ivan Nardini, Jacinda Mein, Jack Zhou, James Svensson, Jeff Stanway, Jetha Chan, Jin Peng Zhou, Joana Carrasqueira, Joana Iljazi, Jocelyn Becker, Joe Fernandez, Joost van Amersfoort, Josh Gordon, Josh Lipschultz, Josh Newlan, Ju yeong Ji, Kareem Mohamed, Kartikeya Badola, Kat Black, Katie Millican, Keelin McDonell, Kelvin Nguyen, Kiranbir Sodhia, Kish Greene, Lars Lowe Sjoesund, Lauren Usui, Laurent Sifre, Lena Heuermann,

- Leticia Lago, Lilly McNealus, Livio Baldini Soares, Logan Kilpatrick, Lucas Dixon, Luciano Martins, Machel Reid, Manvinder Singh, Mark Iverson, Martin Görner, Mat Velloso, Mateo Wirth, Matt Davidow, Matt Miller, Matthew Rahtz, Matthew Watson, Meg Risdal, Mehran Kazemi, Michael Moynihan, Ming Zhang, Minsuk Kahng, Minwoo Park, Mofi Rahman, Mohit Khatwani, Natalie Dao, Nenshad Bardoliwalla, Nesh Devanathan, Neta Dumai, Nilay Chauhan, Oscar Wahltinez, Pankil Botarda, Parker Barnes, Paul Barham, Paul Michel, Pengchong Jin, Petko Georgiev, Phil Culliton, Pradeep Kuppala, Ramona Comanescu, Ramona Merhej, Reena Jana, Reza Ardeshir Rokni, Rishabh Agarwal, Ryan Mullins, Samaneh Saadat, Sara Mc Carthy, Sarah Cogan, Sarah Perrin, Sébastien M. R. Arnold, Sebastian Krause, Shengyang Dai, Shruti Garg, Shruti Sheth, Sue Ronstrom, Susan Chan, Timothy Jordan, Ting Yu, Tom Eccles, Tom Hennigan, Tomas Kocisky, Tulsee Doshi, Vihan Jain, Vikas Yadav, Vilobh Meshram, Vishal Dharmadhikari, Warren Barkley, Wei Wei, Wenming Ye, Woohyun Han, Woosuk Kwon, Xiang Xu, Zhe Shen, Zhitao Gong, Zichuan Wei, Victor Cotruta, Phoebe Kirk, Anand Rao, Minh Giang, Ludovic Peran, Tris Warkentin, Eli Collins, Joelle Barral, Zoubin Ghahramani, Raia Hadsell, D. Sculley, Jeanine Banks, Anca Dragan, Slav Petrov, Oriol Vinyals, Jeff Dean, Demis Hassabis, Koray Kavukcuoglu, Clement Farabet, Elena Buchatskaya, Sebastian Borgeaud, Noah Fiedel, Armand Joulin, Kathleen Kenealy, Robert Dadashi, and Alek Andreev. Gemma 2: Improving open language models at a practical size, 2024. URL <https://arxiv.org/abs/2408.00118>.
- Xavier Glorot and Yoshua Bengio. Understanding the difficulty of training deep feedforward neural networks. In *International Conference on Artificial Intelligence and Statistics*, 2010. URL <https://api.semanticscholar.org/CorpusID:5575601>.
- Zixuan Jiang, Jiaqi Gu, and David Z. Pan. Normsoftmax: Normalizing the input of softmax to accelerate and stabilize training. In *2023 IEEE International Conference on Omni-layer Intelligent Systems (COINS)*, pp. 1–6, 2023. doi: 10.1109/COINS57856.2023.10189242.
- Anemily Machina and Robert Mercer. Anisotropy is not inherent to transformers. In Kevin Duh, Helena Gomez, and Steven Bethard (eds.), *Proceedings of the 2024 Conference of the North American Chapter of the Association for Computational Linguistics: Human Language Technologies (Volume 1: Long Papers)*, pp. 4892–4907, Mexico City, Mexico, June 2024. Association for Computational Linguistics. doi: 10.18653/v1/2024.naacl-long.274. URL <https://aclanthology.org/2024.naacl-long.274>.
- Guilherme Penedo, Hynek Kydlíček, Anton Lozhkov, Margaret Mitchell, Colin A Raffel, Leandro Von Werra, Thomas Wolf, et al. The fineweb datasets: Decanting the web for the finest text data at scale. *Advances in Neural Information Processing Systems*, 37:30811–30849, 2024.
- Tomer Porian, Mitchell Wortsman, Jenia Jitsev, Ludwig Schmidt, and Yair Carmon. Resolving discrepancies in compute-optimal scaling of language models, 2024. URL [https://proceedings.neurips.cc/paper\\_files/paper/2024/file/b6341525cd84f3be0ef203e4d7cd8556-Paper-Conference.pdf](https://proceedings.neurips.cc/paper_files/paper/2024/file/b6341525cd84f3be0ef203e4d7cd8556-Paper-Conference.pdf).
- Ofir Press and Lior Wolf. Using the output embedding to improve language models. In Mirella Lapata, Phil Blunsom, and Alexander Koller (eds.), *Proceedings of the 15th Conference of the European Chapter of the Association for Computational Linguistics: Volume 2, Short Papers*, pp. 157–163, Valencia, Spain, April 2017. Association for Computational Linguistics. URL <https://aclanthology.org/E17-2025/>.
- Alec Radford, Karthik Narasimhan, Tim Salimans, Ilya Sutskever, et al. Improving language understanding by generative pre-training. 2018.
- Alec Radford, Jeff Wu, Rewon Child, David Luan, Dario Amodei, and Ilya Sutskever. Language models are unsupervised multitask learners. 2019. URL <https://api.semanticscholar.org/CorpusID:160025533>.
- Noam Shazeer. Glu variants improve transformer. *arXiv preprint arXiv:2002.05202*, 2020.
- Felix Stollenwerk and Tobias Stollenwerk. Better embeddings with coupled Adam. In Wanxiang Che, Joyce Nabende, Ekaterina Shutova, and Mohammad Taher Pilehvar

- (eds.), *Proceedings of the 63rd Annual Meeting of the Association for Computational Linguistics (Volume 1: Long Papers)*, pp. 27219–27236, Vienna, Austria, July 2025. Association for Computational Linguistics. ISBN 979-8-89176-251-0. doi: 10.18653/v1/2025.acl-long.1321. URL <https://aclanthology.org/2025.acl-long.1321/>.
- Sho Takase, Shun Kiyono, Sosuke Kobayashi, and Jun Suzuki. Spike no more: Stabilizing the pre-training of large language models. In *Second Conference on Language Modeling*, 2025. URL <https://openreview.net/forum?id=52YBEzcI0l>.
- Team OLMo and Allen Institute for AI. Olmo 3: Charting a path through the model flow to lead open-source ai. Technical report, Allen Institute for AI, November 2025. URL <https://allenai.org/blog/olmo3>.
- Team OLMo, Pete Walsh, Luca Soldaini, Dirk Groeneveld, Kyle Lo, Shane Arora, Akshita Bhagia, Yuling Gu, Shengyi Huang, Matt Jordan, Nathan Lambert, Dustin Schwenk, Oyvind Tafjord, Taira Anderson, David Atkinson, Faeze Brahman, Christopher Clark, Pradeep Dasigi, Nouha Dziri, Allyson Ettinger, Michal Guerquin, David Heineman, Hamish Ivison, Pang Wei Koh, Jiacheng Liu, Saumya Malik, William Merrill, Lester James V. Miranda, Jacob Morrison, Tyler Murray, Crystal Nam, Jake Poznanski, Valentina Pyatkin, Aman Rangapur, Michael Schmitz, Sam Skjonsberg, David Wadden, Christopher Wilhelm, Michael Wilson, Luke Zettlemoyer, Ali Farhadi, Noah A. Smith, and Hannaneh Hajishirzi. 2 olmo 2 furious, 2025. URL <https://arxiv.org/abs/2501.00656>.
- Ashish Vaswani, Noam Shazeer, Niki Parmar, Jakob Uszkoreit, Llion Jones, Aidan N Gomez, Łukasz Kaiser, and Illia Polosukhin. Attention is all you need. *Advances in neural information processing systems*, 30, 2017.
- Lingxiao Wang, Jing Huang, Kevin Huang, Ziniu Hu, Guangtao Wang, and Quanquan Gu. Improving neural language generation with spectrum control. In *International Conference on Learning Representations*, 2020. URL <https://api.semanticscholar.org/CorpusID:211145667>.
- Thomas Wang, Adam Roberts, Daniel Hesslow, Teven Le Scao, Hyung Won Chung, Iz Beltagy, Julien Launay, and Colin Raffel. What language model architecture and pretraining objective works best for zero-shot generalization? In Kamalika Chaudhuri, Stefanie Jegelka, Le Song, Csaba Szepesvari, Gang Niu, and Sivan Sabato (eds.), *Proceedings of the 39th International Conference on Machine Learning*, volume 162 of *Proceedings of Machine Learning Research*, pp. 22964–22984. PMLR, 17–23 Jul 2022. URL <https://proceedings.mlr.press/v162/wang22u.html>.
- Mitchell Wortsman, Peter J. Liu, Lechao Xiao, Katie Everett, Alex Alemi, Ben Adlam, John D. Co-Reyes, Izzeddin Gur, Abhishek Kumar, Roman Novak, Jeffrey Pennington, Jascha Sohl-dickstein, Kelvin Xu, Jaehoon Lee, Justin Gilmer, and Simon Kornblith. Small-scale proxies for large-scale transformer training instabilities, 2023. URL <https://arxiv.org/abs/2309.14322>.
- Aiyuan Yang, Bin Xiao, Bingning Wang, Borong Zhang, Ce Bian, Chao Yin, Chenxu Lv, Da Pan, Dian Wang, Dong Yan, Fan Yang, Fei Deng, Feng Wang, Feng Liu, Guangwei Ai, Guosheng Dong, Haizhou Zhao, Hang Xu, Haoze Sun, Hongda Zhang, Hui Liu, Jiaming Ji, Jian Xie, JunTao Dai, Kun Fang, Lei Su, Liang Song, Lifeng Liu, Liyun Ru, Luyao Ma, Mang Wang, Mickel Liu, MingAn Lin, Nuolan Nie, Peidong Guo, Ruiyang Sun, Tao Zhang, Tianpeng Li, Tianyu Li, Wei Cheng, Weipeng Chen, Xiangrong Zeng, Xiaochuan Wang, Xiaoxi Chen, Xin Men, Xin Yu, Xuehai Pan, Yanjun Shen, Yiding Wang, Yiyu Li, Youxin Jiang, Yuchen Gao, Yupeng Zhang, Zenan Zhou, and Zhiying Wu. Baichuan 2: Open large-scale language models, 2025. URL <https://arxiv.org/abs/2309.10305>.
- Zhong Zhang, Chongming Gao, Cong Xu, Rui Miao, Qinli Yang, and Junming Shao. Revisiting representation degeneration problem in language modeling. In Trevor Cohn, Yulan He, and Yang Liu (eds.), *Findings of the Association for Computational Linguistics: EMNLP 2020*, pp. 518–527, Online, November 2020. Association for Computational Linguistics. doi: 10.18653/v1/2020.findings-emnlp.46. URL <https://aclanthology.org/2020.findings-emnlp.46>.

|                              |  |
|------------------------------|--|
| optimizer                    | AdamW  |
| $\beta_1$                    | 0.9  |
| $\beta_2$                    | 0.95   |
| $\epsilon$                   | 1e-8   |
| weight decay                 | 0.0  |
| gradient clipping            | 1.0  |
| dropout                      | 0.0  |
| <b>weight tying</b>          | <b>false &amp; true (false)</b>  |
| qk-layernorm                 | yes  |
| bias                         | no   |
| learning rate schedule       | cosine decay   |
| learning rate minimum        | 1e-5   |
| layer normalization          | LayerNorm  |
| precision                    | BF16   |
| positional embedding         | RoPE   |
| <b>vocab size</b>            | <b>50304 (32101)</b>   |
| <b>hidden activation</b>     | <b>SwiGLU (GeLU)</b>   |
| <b>sequence length</b>       | <b>2048 (512)</b>  |
| <b>batch size (samples)</b>  | <b>64 (256)</b>  |
| batch size (tokens)          | 131072   |
| training length              | 100000 steps $\approx$ 13.1B tokens  |
| warmup                       | 5000 steps $\approx$ 0.7B tokens   |
| embedding initialization     | Normal with standard deviation $1/\sqrt{d}$                                      |
| <b>weight initialization</b> | <b>Xavier with average of fan.in and fan.out (Xavier with fan.in, truncated)</b> |

Table 4: Architectural details and hyperparameters used in all our experiments. All settings match the ones from [Wortsman et al. \(2023\)](#), with six exceptions. These are highlighted in bold, with the choice from [Wortsman et al. \(2023\)](#) being specified in parentheses.

## A Hyperparameters

All our experiments use the architecture and hyperparameters specified in Tab. 4.

## B Proof of Theorem 4

**Theorem 4.** Let  $B_-, B_+ \in \mathbb{R}$  be bounds such that

$$\|\mu\|^2 - B_- \leq e_i \cdot \mu \leq \|\mu\|^2 + B_+ \quad (12)$$

where  $\mu$  represents the mean output embedding. Define the (non-negative) ratio

$$B_{\text{ratio}} = \frac{\max(B_-, B_+)}{\max(B_- - \|\mu\|^2, B_+ + \|\mu\|^2)} \quad (13)$$

and denote the output logits after  $\mu$ -centering by  $l_i^*$ . Then

$$B_{\text{ratio}} \leq 1 \iff \max |l_i^*| \leq \max |l_i| \quad (14)$$

*Proof.* Denote the output embeddings after  $\mu$ -centering by  $e_i^*$ . The bounds of  $e_i^* \cdot \mu$  are

$$-B_- \leq e_i^* \cdot \mu \leq B_+ \quad (24)$$

From Eq. (12) and Eq. (24) we conclude that the respective bounds for the maximum of the absolute values of the dot products are

$$\begin{aligned} \max_i |e_i \cdot \mu| &= \max(B_- - \|\mu\|^2, B_+ + \|\mu\|^2) \\ \max_i |e_i^* \cdot \mu| &= \max(B_-, B_+) \end{aligned} \quad (25)$$

respectively. Hence, Eq. (13) can be written as

$$B_{\text{ratio}} = \frac{\max_i |e_i^* \cdot \mu|}{\max_i |e_i \cdot \mu|} \quad (26)$$

We will first prove the sufficiency ( $\Rightarrow$ ) part of Eq. (14).  $B_{\text{ratio}} \leq 1$  is equivalent to

$$\max_i |e_i^* \cdot \mu| \leq \max_i |e_i \cdot \mu| \quad (27)$$

which can also be written as

$$\max_i |e_i^* \cdot \hat{\mu}| \leq \max_i |e_i \cdot \hat{\mu}| \quad (28)$$

with the unit vector  $\hat{\mu} = \mu / \|\mu\|$ . Let us now consider  $e_i^*$  and decompose it into the sum

$$e_i^* = e_i^{*\parallel} + e_i^{*\perp} \quad (29)$$

of two vectors

$$e_i^{*\parallel} = (e_i^* \cdot \hat{\mu}) \cdot \hat{\mu} \quad (30)$$

$$e_i^{*\perp} = e_i^* - (e_i^* \cdot \hat{\mu}) \cdot \hat{\mu} \quad (31)$$

parallel and perpendicular to the mean embedding. This leads to

$$\begin{aligned} \max_i \|e_i^*\|^2 &= \max_i \|e_i^{*\parallel} + e_i^{*\perp}\|^2 \\ &= \max_i \|e_i^{*\parallel}\|^2 + \max_i \|e_i^{*\perp}\|^2 \end{aligned} \quad (32)$$

since  $e_i^{*\parallel} \cdot e_i^{*\perp} = 0$ . The same decomposition can be conducted for  $e_i$ . However, the perpendicular component is not affected by  $\mu$ -centering,  $e_i^{*\perp} = e_i^\perp$ , and neither is the second summand in Eq. (32). Hence, we can write

$$\begin{aligned} &\max_i \|e_i^*\|^2 - \max_i \|e_i\|^2 \\ &= \max_i \|e_i^{*\parallel}\|^2 - \max_i \|e_i^\parallel\|^2 \\ &= \max_i |e_i^* \cdot \hat{\mu}| - \max_i |e_i \cdot \mu| \\ &\leq 0 \end{aligned} \quad (33)$$

where in the last two steps, Eq. (30) and Eq. (27) were used, respectively. Thus,

$$\max_i \|e_i^*\|^2 \leq \max_i \|e_i\|^2 \quad (34)$$

The same holds for the (non-squared) norm of the mean embedding, which in turn leads to the right hand side of Eq. (14) via Lemma 2:

$$\max_i |l_i^*| \leq \max_i |l_i| \quad (35)$$

The proof for the necessity ( $\Leftarrow$ ) part of Eq. (14) can be obtained by reversing the logic from Eq. (27) to Eq. (35).  $\square$

### C Results for $B_{\text{ratio}}$

As described in Sec. 3, we trained a total of 70 baseline models with a standard language modeling head (see Sec. 1), using 7 different learning rates (see Eq. (19)), 5 different model sizes (see Eq. (20)) and the 2 possible choices regarding weight tying (see Eq. (21)). Tab. 5 lists  $B_{\text{ratio}}$ , as defined in Eq. (14), individually for each of these models, while Fig. 5 shows histograms of all its values. For each model in the absence of weight tying, we find that the condition for Theorem 4 is fulfilled:  $B_{\text{ratio}} \leq 1$ . In the presence of weight tying, we observe a similar behavior, with two differences: the values of  $B_{\text{ratio}}$  are generally larger, and even exceed the threshold  $B_{\text{ratio}} = 1$  in 4 out of 35 cases with the lowest learning rate. However, as can be seen in Tab. 6 and Fig. 8 (see App. E), these particular training runs are very stable anyway, both for the baseline and any employed mitigation strategy. Finally, Tab. 5 also shows that  $B_{\text{ratio}}$  tends to decrease with a larger learning rate. This indicates that the beneficial effect of  $\mu$ -centering (or  $\mu$ -loss) on the output logit bounds becomes larger, which is also in accordance with our results in Sec. 4.

| weight tying = false |      |      |      |      |      |      |      | weight tying = true |      |      |      |      |      |      |      |
|----------------------|------|------|------|------|------|------|------|---------------------|------|------|------|------|------|------|------|
| $N$                  | 3e-4 | 1e-3 | 3e-3 | 1e-2 | 3e-2 | 1e-1 | 3e-1 | $N$                 | 3e-4 | 1e-3 | 3e-3 | 1e-2 | 3e-2 | 1e-1 | 3e-1 |
| 4                    | 0.97 | 0.82 | 0.75 | 0.62 | 0.66 | 0.26 | 0.65 | 4                   | 1.12 | 0.77 | 0.85 | 0.78 | 0.71 | 0.54 | 0.58 |
| 6                    | 0.98 | 0.82 | 0.92 | 0.73 | 0.49 | 0.30 | 0.44 | 6                   | 1.11 | 0.94 | 0.65 | 0.84 | 0.59 | 0.60 | 0.60 |
| 8                    | 0.96 | 0.81 | 0.79 | 0.67 | 0.60 | 0.66 | 0.57 | 8                   | 1.16 | 0.77 | 0.85 | 0.79 | 0.67 | 0.66 | 0.71 |
| A                    | 0.97 | 0.74 | 0.67 | 0.74 | 0.72 | 0.61 | 0.70 | A                   | 1.08 | 0.84 | 0.90 | 0.76 | 0.70 | 0.60 | 0.70 |
| C                    | 0.95 | 0.74 | 0.84 | 0.91 | 0.68 | 0.70 | 0.70 | C                   | 0.94 | 0.82 | 0.80 | 0.76 | 0.72 | 0.67 | 0.77 |

Table 5:  $B_{\text{ratio}}$  for all baseline models with a standard language modeling head. The numbers in the column header represent the learning rate  $\eta$ . The results are shown separately for the absence (left) and presence (right) of weight tying.

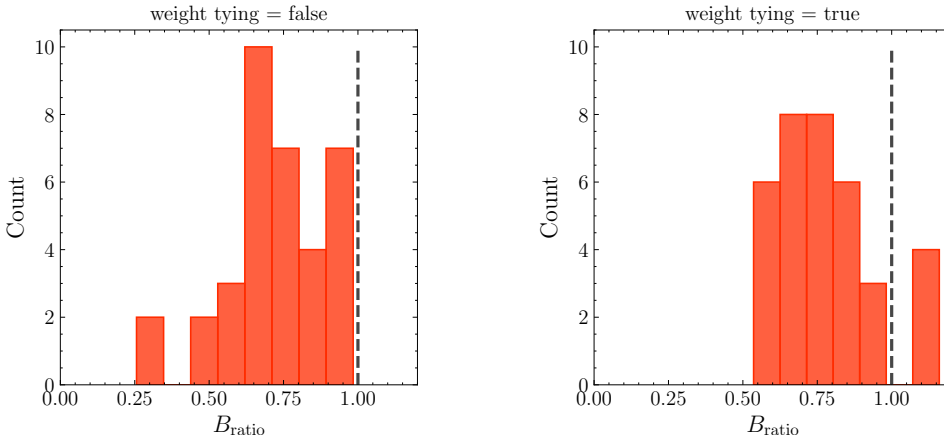


Figure 5: Histogram of  $B_{\text{ratio}}$  for all baseline models with a standard language modeling head. The results are shown separately for the absence (left) and presence (right) of weight tying.

## D Illustrations for z-loss

Fig. 6 shows  $\mathcal{L}_z$  as a function of a single logit  $l_i$ , see Eq. (17), for 3 different values of  $S = \sum_{j \neq i} \exp(l_j)$ . It illustrates that the function is even only for the theoretical edge case of  $S = 0$ , corresponding to  $\lim l_j \rightarrow -\infty$  for all  $j \neq i$ . The fact that z-loss treats positive and negative logits differently is also evident from Fig. 7. It shows  $Z$  and  $\mathcal{L}_z$  for a toy example of two logits,  $l_1$  and  $l_2$ . Neither function is invariant under the transformation  $l_i \rightarrow -l_i$  (i.e. a  $180^\circ$  rotation around the z-axis). In fact, the limit  $\mathcal{L}_z \rightarrow \infty$ , which corresponds to either  $Z \rightarrow 0$  or  $Z \rightarrow \infty$ , is approached differently: while  $Z \rightarrow 0$  requires *all* logits to diverge negatively,  $Z \rightarrow \infty$  is obtained if *any* logit diverges positively.

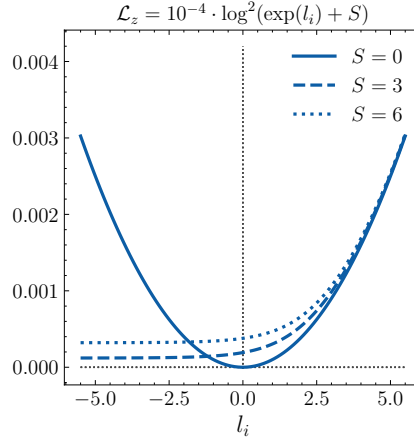


Figure 6: Illustration of  $\mathcal{L}_z$  as a function of a single logit  $l_i$  as given by Eq. (17), for 3 different values of  $S = \sum_{j \neq i} \exp(l_j)$ .

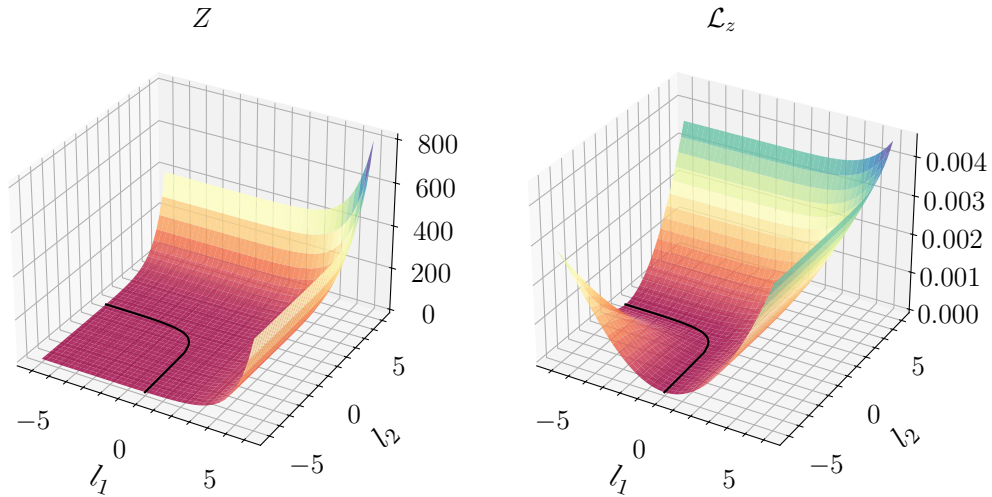


Figure 7: The quantities  $Z$  (left, Eq. (4)) and  $\mathcal{L}_z$  (right, Eq. (5)) as a function of two logits, i.e.  $V = 2$ . The black curves represent the z-loss optimum,  $Z = 1$  and  $\mathcal{L}_z = 0$ .

| (i) Optimal Loss ( $\downarrow$ ) |             |             |             |             |              |
|-----------------------------------|-------------|-------------|-------------|-------------|--------------|
| $N$                               | baseline    | soft-c.     | z-loss      | $\mu$ -loss | $\mu$ -cent. |
| 16M                               | <b>3.83</b> | <b>3.83</b> | <b>3.83</b> | <b>3.83</b> | <b>3.83</b>  |
| 29M                               | <b>3.56</b> | <b>3.56</b> | <b>3.56</b> | <b>3.56</b> | <b>3.56</b>  |
| 57M                               | 3.34        | <b>3.33</b> | <b>3.33</b> | 3.34        | 3.34         |
| 109M                              | 3.16        | <b>3.15</b> | <b>3.15</b> | 3.16        | 3.16         |
| 221M                              | <b>3.00</b> | <b>3.00</b> | <b>3.00</b> | <b>3.00</b> | 3.01         |

| (ii) Learning Rate Sensitivity ( $\downarrow$ ) |          |              |        |              |              |
|---|----------|--------------|--------|--------------|--------------|
| $N$   | baseline | soft-c.      | z-loss | $\mu$ -loss  | $\mu$ -cent. |
| 16M   | 0.050    | 0.041        | 0.056  | <b>0.022</b> | 0.034        |
| 29M   | 0.061    | 0.030        | 0.042  | <b>0.026</b> | 0.042        |
| 57M   | 0.308    | <b>0.031</b> | 0.103  | 0.038        | 0.042        |
| 109M  | 0.335    | <b>0.049</b> | 0.083  | 0.053        | 0.061        |
| 221M  | 0.330    | <b>0.055</b> | 0.109  | 0.058        | 0.066        |

| (iii) Additional Training Time ( $\downarrow$ ) |          |         |        |             |              |
|---|----------|---------|--------|-------------|--------------|
| $N$   | baseline | soft-c. | z-loss | $\mu$ -loss | $\mu$ -cent. |
| 16M   | 0.0%     | 11.2%   | 6.6%   | <b>0.5%</b> | 0.7%         |
| 29M   | 0.0%     | 7.1%    | 4.0%   | <b>0.4%</b> | 0.5%         |
| 57M   | 0.0%     | 4.5%    | 2.7%   | 0.8%        | <b>0.7%</b>  |
| 109M  | 0.0%     | 2.8%    | 1.8%   | <b>0.4%</b> | 0.6%         |
| 221M  | 0.0%     | 1.4%    | 1.0%   | <b>0.0%</b> | 0.2%         |

Table 6: Main results for all model sizes and variants using weight tying. *From top to bottom:* (i) Optimal loss,  $\min_{\eta} \mathcal{L}$ . (ii) Learning rate sensitivity, LRS. (iii) Additional training time relative to baseline. In (i) and (ii), the best result for each model size is highlighted in bold. The same is true for (iii), where the baseline is excluded from the comparison though.

## E Results for Weight Tying

The main results of our experiments with weight tying are shown in Tab. 6 and Fig. 8. They are very similar to their counterparts without weight tying, see Tab. 2 and Fig. 2.

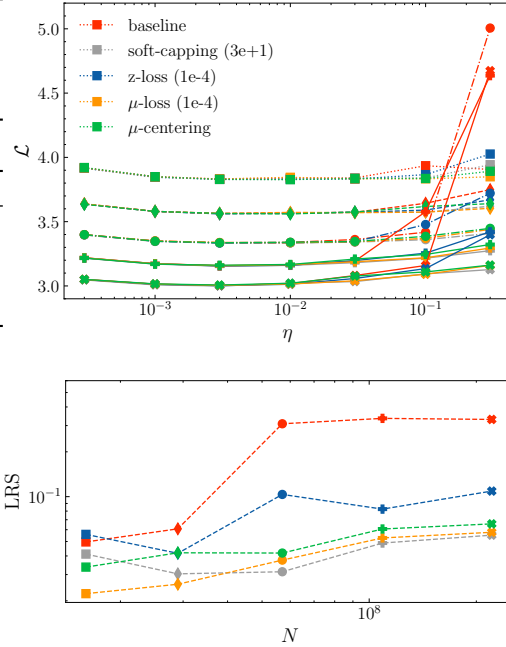


Figure 8: Main results for all model sizes  $N$  and variants using weight tying. *Top:* Dependency of the loss  $\mathcal{L}$  on the learning rate  $\eta$ . *Bottom:* Dependency of the learning rate sensitivity LRS on the model size  $N$ .